NASA TECHNICAL NOTE

NASA TN D-4188

NASA TN D-4188

EXPERIMENTAL INVESTIGATION OF BOUNDARY-LAYER TRANSITION ON A COOLED 7.5° TOTAL-ANGLE CONE AT MACH 10

by Philip E. Everhart and H. Harris Hamilton

Langley Research Center
Langley Station, Hampton, Va.

NATIONAL AERONAUTICS AND SPACE ADMINISTRATION • WASHINGTON, D. C. • OCTOBER 1967

NASA TN D-4188

EXPERIMENTAL INVESTIGATION OF BOUNDARY-LAYER TRANSITION ON A COOLED 7.5° TOTAL-ANGLE CONE AT MACH 10

By Philip E. Everhart and H. Harris Hamilton

Langley Research Center
Langley Station, Hampton, Va.

NATIONAL AERONAUTICS AND SPACE ADMINISTRATION

For sale by the Clearinghouse for Federal Scientific and Technical Information
Springfield, Virginia 22151 – CFSTI price $3.00

EXPERIMENTAL INVESTIGATION OF BOUNDARY-LAYER TRANSITION ON A COOLED 7.5° TOTAL-ANGLE CONE AT MACH 10

By Philip E. Everhart and H. Harris Hamilton
Langley Research Center

SUMMARY

An experimental investigation of boundary-layer transition was conducted on a cooled 7.5° total-angle cone at a free-stream Mach number of 10 and a free-stream unit Reynolds number range of 0.4×10^6 to 2.2×10^6 per foot (1.3×10^6 to 7.2×10^6 per meter). Local unit Reynolds numbers from 0.7×10^6 to 3.1×10^6 per foot (2.3×10^6 to 10.2×10^6 per meter) were obtained at a local Mach number of approximately 9.

At a local Mach number of approximately 9, transition Reynolds number was found to be essentially independent of wall temperature for the ratios of wall temperature to adiabatic wall temperature of the investigation $\left(0.42 \leqq \frac{T_w}{T_{aw}} \leqq 0.63\right)$. Local transition Reynolds number increases with local unit Reynolds number. The increase in transition Reynolds number (based on the end of transition) with local Mach number that has been noted at moderate supersonic Mach numbers continued to a local Mach number of approximately 9.

INTRODUCTION

Transition of the boundary layer assumes added importance at hypersonic speeds because of the effects on convective heating as well as on skin friction. Although a number of studies of boundary-layer transition at hypersonic speeds have appeared in the literature (for example, refs. 1 to 6), no reliable method has emerged for predicting when transition will occur. Thus, the values of transition Reynolds number must be estimated from correlations of available experimental data. Useful correlations are particularly difficult to obtain because of the large number of parameters which can affect transition. (See ref. 2.) Recent experimental data concerning the effect of wall cooling, nose bluntness, and roughness elements on the transition of the hypersonic boundary layer on a slender cone are presented in reference 7. The results and analyses of an investigation conducted in the Langley continuous-flow hypersonic tunnel on a sharp cone with varying wall temperature are presented herein.

The purpose of the present test was to determine the beginning and the end of transition on a 7.5° total-angle cone at a nominal free-stream Mach number of 10. Transition was detected by means of heat-transfer measurements. The cone was tested at an angle of attack of 0° for free-stream unit Reynolds numbers from about 0.4×10^6 to 2.2×10^6 per foot (1.31×10^6 to 7.22×10^6 per meter). The stream stagnation temperature was about 1815° R (1008° K) and the tunnel stagnation pressure was varied from 300 to 1800 pounds per square inch absolute (21×10^5 to 124×10^5 newtons/meter^2).

SYMBOLS

c_p specific heat of gas at constant pressure

c_w specific heat of wall material

C constant in power law relation

h heat-transfer coefficient, $\frac{q}{T_{aw} - T_w}$

k thermal conductivity

L length of cone

M Mach number

n exponent in power law relation

N_{Pr} Prandtl number

N_{St} Stanton number, $\frac{h}{\rho_\infty u_\infty c_{p,\infty}}$

p pressure

q rate of heat flow per unit area

q_c net rate of heat flow resulting from conduction per unit surface area

r radius

R Reynolds number, $\frac{\rho u x}{\mu}$

S	distance along cone surface (table I)
T	absolute temperature
t	time
u	velocity
x	distance along cone center line measured from apex
γ	ratio of specific heats, 1.4
ϵ	emissivity
η	recovery factor
θ	cone half-angle
μ	dynamic viscosity
ρ	density
σ	Stefan-Boltzmann constant
τ	thickness of wall
τ_e	effective skin thickness
ϕ	peripheral angle measured from top ray

Subscripts:

aw	adiabatic wall
b	beginning of transition
l	local
t	stagnation
tr	transition

w wall

∞ free stream

Primes denote parameters evaluated at reference-temperature conditions.

FACILITY

The investigation was conducted in the Langley continuous-flow hypersonic tunnel which operates at free-stream Mach numbers that vary almost linearly from 10.13 at 300 psia (21×10^5 N/m^2) to 10.32 at 1500 psia (103×10^5 N/m^2). A photograph of the facility is shown in figure 1. This facility is capable of continuously maintaining a prescribed set of test conditions by recirculating the test air through a series of compressors. The test air is heated to avoid liquefaction by an electrical resistance tube heater and then expanded through a contoured, three-dimensional, water-cooled nozzle to test conditions in a 31-inch-square (78.7 cm) test section. A sketch of the cone installed in the test section is shown in figure 2.

MODEL

The model used in the investigation was a sharp-tip right-circular cone with a total angle of 7.5°, a length of 69.38 inches (176.2 cm) measured from the vertex along the axis of symmetry, and a base diameter of 9 inches (22.86 cm). The tip diameter at the beginning of the test was 0.004 inch (0.0102 cm). At the completion of the test, the tip diameter was again measured and found to be 0.010 inch (0.025 cm). A photograph of the sharp tip cone is shown in figure 3(a). The cone was made from 347 stainless steel in three sections (fig. 3(b)) to facilitate installation of the instrumentation; the sections were welded together and the surface was ground and hand polished to a nominal surface finish of approximately 6 microinches (152 nanometers). The joints between sections were carefully faired smooth in an attempt to eliminate any effect of surface irregularities on the flow field. The cone wall thickness was approximately 0.25 inch (0.635 cm).

In order to vary the ratio of wall temperature to stagnation temperature, the cone was equipped with an internal cooling system utilizing gaseous nitrogen. The gaseous nitrogen entered the cone through the sting mount and was distributed inside by a coolant tube shown in a cross section of the cone in figure 4. Jets from this tube cooled the forward portion of the cone; whereas an internal conical shell caused the coolant to fan out and cool the rearward portion. After passing through the cone, the coolant was exhausted through the tunnel strut into the atmosphere.

Instrumentation

The cone was instrumented with 116 thermocouples for the measurement of model temperatures and 21 pressure orifices for the measurement of surface static pressures. The locations of the thermocouples and pressure orifices are given in table I. Number 30 gage chromel-alumel thermocouples (0.010 inch diameter (0.025 cm)) were installed in five rows along the model surface beginning 13 inches (33.02 cm) from the tip of the cone. Details of the thermocouple installation are shown in figure 4. The chromel-alumel wires were separated by magnesium oxide insulation and covered by a 0.065-inch (0.165 cm) outside diameter inconel sheath. Outside the model, fiber-glass-insulated thermocouple wire was soldered to the inconel-sheathed wire and the leads directed through the model support system to the recording system outside the tunnel. Thermocouple outputs were automatically recorded on magnetic tape by an analog-to-digital converter. The reference junction of each thermocouple was maintained at 125° F (325° K).

The 0.040-inch-diameter (0.102 cm) pressure orifices were installed aft of the 15-inch-chord (38.10 cm) station and were primarily located along the bottom ray of the cone ($\phi = 180^{\circ}$). Several pressure orifices were installed along other rays to provide a check on the symmetry of the flow. The pressure leads were directed through the cone support system to a measuring and recording system outside the tunnel. The pressures were measured by means of ionization gages utilizing a small radioactive source to ionize a gas sample. In the range from 1 to 30 mm of mercury, the gage is accurate to ±2 percent of the reading. Below 1 mm of mercury, the accuracy is ±5 percent of the gage reading. The measured pressures were recorded by means of an analog-to-digital data recording system.

Tests and Procedure

All tests were conducted at a nominal free-stream Mach number of 10 and an average stagnation temperature of 1815° R (1008° K). The tunnel stagnation pressure was varied from approximately 300 to 1800 pounds per square inch absolute (21×10^5 to 124×10^5 newtons per square meter). The corresponding range of free-stream unit Reynolds number was from approximately 0.4×10^6 to 2.2×10^6 per foot (1.31×10^6 to 7.22×10^6 per meter). Details of the test conditions are given in table II.

The test procedure consisted of initially cooling the model to the lowest possible temperature. After the desired tunnel condition had been reached, the coolant was turned off and temperature rise rates recorded. The temperature of the model rose so slowly that it was unnecessary to recool the model for each successive stagnation pressure. The model was cooled only when the temperature had risen approximately 300° F (167° K). To observe the effect of wall temperature on transition, the cone was initially

cooled and with no further cooling, surface temperatures were recorded as the cone was allowed to approach a radiation equilibrium temperature.

REDUCTION OF HEAT-TRANSFER DATA

The convective heat-transfer coefficient, defined in terms of the heat input to the cone, was calculated from the temperature-time histories at the thermocouple locations and corrected for radiation to the tunnel walls by using the following equation:

$$q = h\left(T_{aw} - T_w\right) = \rho_w c_w \tau_e \frac{dT_w}{dt} + \epsilon \sigma T_w^4$$

The temperature-time derivative dT_w/dt was determined by first fitting a quadratic least-squares curve to the measured data, differentiating this curve, and then evaluating the result at the desired time. The values of the density ρ_w and specific heat c_w of the wall material were taken to be 0.290 lb/in^3 (0.803×10^4 kg/m^3) and 0.120 Btu/^{o}F-lb (502.1 J/^{o}K-kg), respectively. Values of the effective skin thickness were calculated from the equation $\tau_e = \tau_w - \tau_w^2/2r$ by using the actual skin thickness measured during the construction of the cone. Effective skin thicknesses varied from 0.223 to 0.256 inch (0.566 to 0.650 cm). The large values of cone wall temperature encountered during some runs made it necessary to correct the measured heat-transfer data for radiative heat transfer. The tunnel wall temperature was maintained at a value less than 150^o F (339^o K) and thus the radiative heat transfer from the tunnel wall to the cone was insignificant. The emissivity ϵ of the cone was measured and found to be approximately constant at a value of 0.23 for the range of wall temperatures of interest.

The adiabatic wall temperature was obtained from the equation

$$\frac{T_{aw}}{T_t} = \eta + \frac{T_\infty}{T_t}(1 - \eta)$$

A laminar recovery factor of $\eta = \sqrt{N_{Pr}}$ was used in this equation and the values of T_{aw}/T_t thus calculated were used for both laminar and turbulent flow. The Prandtl number was assumed to be 0.72.

RESULTS AND DISCUSSION

Pressure Distribution

Distributions of the ratios of cone surface pressure to free-stream static pressure p_l/p_∞ are presented in figure 5 for stagnation pressures from 300 to 1500 psia

(21×10^5 to 103×10^5 N/m^2). These measured pressures decrease in a streamwise direction along the cone and are slightly higher than those predicted by inviscid cone theory from Kopal (ref. 8). Most pressures were measured along the bottom ray on the cone ($\phi = 180^o$); however, at two stations ($x/L = 0.288$ and $x/L = 0.432$) pressures were also measured along the top ($\phi = 0^o$) and side rays ($\phi = 90^o$) on the cone. The agreement among these measured radial pressures is good (that is, within the accuracy of the instruments); thus, the flow appears to be symmetrical about the cone axis.

The analysis of all the data on the cone is based on local flow conditions on the surface of the cone. The local flow properties (M_l, p_l, T_l, and R_l) on the cone were obtained by assuming that the flow passed through a conical shock of sufficiently large inclination to raise the pressure to the level of the average measured surface pressure.

Temperature Distribution

The ratio of equilibrium wall temperature to stagnation temperature T_w/T_t is presented in figure 6(a) for stagnation pressures from 300 psia (21×10^5 N/m^2) to 1500 psia (103×10^5 N/m^2). These distributions were obtained on the uncooled cone by operating the tunnel at fixed stagnation conditions until the wall temperatures reached equilibrium. For stagnation pressures at 900 psia (63×10^5 N/m^2) and below, the equilibrium wall temperature decreases in a streamwise direction which is indicative of laminar flow. At higher stagnation pressures the wall temperature is relatively uniform over the forward portion of the cone and increases over the rearward portion; thus, the existence of a region of turbulent flow on the rear of the cone is suggested.

Typical distributions of the ratio of wall temperature to stagnation temperature T_w/T_t are presented in figures 6(b) and 6(c), with time as a parameter, for stagnation pressures of 300 psia (21×10^5 N/m^2) and 1500 psia (103×10^5 N/m^2), respectively. In these cases the cone was first cooled, the coolant flow was then turned off, and the surface temperature was recorded as the cone heated up. At the lower pressure (fig. 6(b)), the temperature immediately after turning off the coolant ($t = 0$ sec) was much higher on the rearward portion of the cone than on the forward portion. Higher initial temperatures on the rearward portion of the cone result from nonuniform cooling of the cone prior to initiation of the test cycle. This initial temperature difference decayed with time and the shape of the temperature distribution slowly tended toward the shape of the equilibrium temperature distribution obtained at this pressure without the initial cooling. (See fig. 6(a).) This change in the temperature distribution with time would be expected for laminar flow over the cone surface. At the higher stagnation pressure (fig. 6(c)), the step increase in temperature on the rearward portion of the cone remains for all times of the test. It will be shown later that a substantial amount of turbulent flow existed on the cone at this stagnation pressure and thus the relatively high heating

rate associated with turbulent flow causes the step in the temperature distribution to be present even for large times after the start of the test (that is, $t = 1546$ seconds).

Because of nonuniform cooling, heat-transfer measurements were made with nonisothermal walls. Estimates of heat conduction along the cone surface were made to determine the error that this effect might introduce in the measured heat-transfer data. The one-dimensional heat conduction in a radial direction along the surface of a cone is given by the equation

$$q_c = k_w \tau_w \left(\frac{d^2 T_w}{dS^2} + \frac{1}{S} \frac{dT_w}{dS} \right)$$

The derivatives in this equation were evaluated by using a three-point finite difference method and a fairing of the measured wall temperature distributions. In general, the heat-conduction corrections were found to be a maximum at the point where the second derivative $\left(d^2T_w/dS^2\right)$ was a maximum (that is, near $x/L = 0.5$ for typical temperature distributions in figures 6(b) and 6(c)). The maximum conduction correction was found to be approximately 10 percent; however, for most of the data, the conduction corrections are less than 5 percent of the measured data. All data are presented without conduction corrections.

TRANSITION REYNOLDS NUMBER

Mach number, unit Reynolds number, and the ratio of wall temperature to adiabatic wall temperature T_w/T_{aw} are among the principal parameters that are known to affect boundary-layer transition. Their effects have been investigated and are discussed in subsequent sections.

Stanton number distributions are compared with those of laminar and turbulent theories (presented in the appendix) to determine the location of transition. The start of transition is taken as the location where the slope of the faired data distributions first deviate significantly from the slope of laminar theory and continue this deviation downstream. The end of transition is taken as the location where the data reach a maximum above turbulent theory. The effect of wall temperature gradient on aerodynamic heating was investigated by the theory of Chapman and Rubesin (ref. 9) and was found to have no effect in determining the start of transition. Since the points at which transition is initiated or completed cannot be precisely defined, arrows are placed on the faired Stanton number distributions to indicate the points selected by the authors as the beginning and end of the transition regions.

Effect of Wall Temperature

In figure 7(a) at a local unit Reynolds number of 2.7×10^6 per foot (8.86×10^6 per meter) both the start and end of the transition region are shown to be essentially independent of T_w/T_{aw} for the range of the investigation $\left(\text{that is, } 0.428 \leqq T_w/T_{aw} \leqq 0.625\right)$. Local transition Reynolds numbers obtained from these data, along with data from several other sources (refs. 7 and 10 to 12), are presented in figure 7(b) as a function of T_w/T_{aw}. Data in the figure at the left are from the hypersonic speed region $\left(M_l \geqq 5\right)$ and those at the right are from the supersonic speed region $\left(1 \leqq M_l \leqq 5\right)$.

The temperature ratio T_w/T_{aw} associated with transition for the present data was obtained from the wall temperature at the beginning of the transition region. It was found that at this local unit Reynolds number, transition on the surface always started ahead of the strong temperature gradient (fig. 6(c)), where the wall temperature was relatively uniform. Many parameters are known to affect transition; thus, when data are compared to determine the effect of T_w/T_{aw}, it is necessary to select data that are compatible with respect to other parameters. The transition data that are compared with the present data in figure 7(b) are restricted to those taken on sharp cones at an angle of attack of 0^o and at approximately the same local Mach number and local unit Reynolds number. These hypersonic data indicate that wall temperature in the range of 10 to 60 percent of adiabatic wall temperature have no significant effect on local transition Reynolds number. This behavior at hypersonic local Mach numbers is very different from that observed at lower supersonic local Mach numbers (see right-hand side of fig. 7(b)). Nagamatsu et al. (ref. 13) suggests that the explanation for this phenomenon lies in the movement of the critical layer to the outer edge of the boundary layer at high Mach numbers. Thus, the low-density fluid that exists in the region of the boundary layer near the wall at high Mach numbers restricts the influence of wall temperature on the transition process.

Effect of Local Unit Reynolds Number

The Stanton number distributions for the complete range of stagnation pressures of the test are presented in figure 8. These distributions were used to determine the effect of local unit Reynolds number on the location of the beginning and end of transition. The lowest local unit Reynolds number for which the start of transition can be identified is 1.26×10^6 per foot (4.13×10^6 per meter). (See fig. 8(b).) At lower local unit Reynolds numbers the data indicate that transition may be occurring toward the rear of the cone; however, the deviation of the slope of the faired data from that of laminar theory is not significant enough to identify the start of transition. At higher local unit Reynolds numbers the location of the start of transition tends to move forward on the cone surface. Transition does not end on the cone until the local unit Reynolds number

is 1.72×10^6 per foot (5.64×10^6 per meter). (See fig. 8(b).) With further increases in local unit Reynolds number the location of the end of transition also tends to move forward on the cone. A difference in the heating on the lower ray ($\phi = 180^o$) is noted in figure 8(c). However, these data still generally indicate that the flow is turbulent and thus do not change any of the previous results.

The transition locations and local unit Reynolds numbers from figures 7(a) and 8 have been used in figure 9 to determine the effect of local unit Reynolds number on local transition Reynolds number. These data indicate that local transition Reynolds number (based on both beginning and end of transition) increases with unit Reynolds number. Power law relations of the form $R_{l,tr} = C\left(R_{l/ft}\right)^n$ were fitted to the data by the method of least squares. These results indicate that local transition Reynolds number is related to local unit Reynolds number by the relation $R_{l,tr} \propto \left(R_{l/ft}\right)^{0.35}$ for transition Reynolds numbers based on the beginning of transition and by $R_{l,tr} \propto \left(R_{l/ft}\right)^{0.45}$ for transition Reynolds numbers based on the end of transition.

Since the transition region is not subject to precise definition, some variation in the two exponents would be anticipated. However, these values are consistent with those of James (ref. 14), who found that for a flat plate, transition Reynolds number increases approximately as the 0.4 power of unit Reynolds number. A similar power law relation with $n \approx 0.35$ was found by the present authors to correlate the data of Potter and Whitfield (ref. 15) which were also obtained on sharp cones at hypersonic Mach numbers.

Effect of Local Mach Number

The present data are compared with published data (refs. 7, 15, 16, 17, and 18) at lower Mach numbers in figure 10 to determine the effect of local Mach number on local transition Reynolds number. The data used for comparison were carefully selected in an attempt to minimize the influence of other parameters on transition. The data were all obtained on sharp cones of small half-angle ($\theta < 5^o$) at an angle of attack of 0^o. The data were also obtained at a local unit Reynolds number of approximately 2.4×10^6 per foot (7.87×10^6 per meter) except for those of Potter and Whitfield (ref. 15) which were adjusted to a unit Reynolds number of 2.4×10^6 per foot (7.87×10^6 per meter) by using the relation $R_{tr} \propto \left(R/ft\right)^{0.35}$ (see preceding section). At lower local Mach numbers where T_w/T_{aw} is known to affect transition, the data were all obtained at near adiabatic wall conditions. The present data and that of Sanator et al. (ref. 7) were obtained under conditions of extreme boundary-layer cooling; however, in both cases T_w/T_{aw} did not affect local transition Reynolds number over the range of T_w/T_{aw} from 0.10 to 0.63. Thus, it is assumed that these results can be extrapolated to near adiabatic wall conditions. The transition Reynolds numbers presented in figure 10 are also limited to

those that should correlate reasonably well with transition Reynolds numbers based on the distance to the end of transition.

The data in figure 10 thus represent the qualitative effect of local Mach number on local transition Reynolds number (based on the end of transition) on a sharp cone at an angle of attack of 0° and near adiabatic wall conditions. The data show that local transition Reynolds number decreases with increasing local Mach number to a minimum at $M_l \approx 3.6$. Beyond this point, local transition Reynolds number increases for high supersonic local Mach numbers. The present data indicate that this increase in local transition Reynolds number continues to a local Mach number of approximately 9. This increase in transition Reynolds number with local Mach number (in the hypersonic region) is also shown by Potter and Whitfield (ref. 15) and Sanator et al. (ref. 7) but is in contrast with the results of Stainback (ref. 6).

CONCLUSIONS

From this investigation of boundary-layer transition on a 7.5° total-angle cone in the Langley continuous-flow hypersonic tunnel at a nominal Mach number of 10 and over a free-stream unit Reynolds number range from 0.4×10^6 to 2.2×10^6 per foot (1.31×10^6 to 7.22×10^6 per meter), it is concluded that:

1. At a local Mach number of approximately 9, local transition Reynolds numbers are essentially independent of wall temperature for ratios of wall temperature to adiabatic wall temperature from 0.42 to 0.63.

2. Local transition Reynolds number increases with local unit Reynolds number.

3. The increase in transition Reynolds number (based on the end of transition) with local Mach number that has been noted at moderate supersonic Mach numbers continues to a local Mach number of approximately 9.

Langley Research Center,
National Aeronautics and Space Administration,
Langley Station, Hampton, Va., March 17, 1967,
129-01-08-42-23.

APPENDIX

HEAT-TRANSFER THEORIES

Laminar Strip Theory

The laminar heat-transfer correlating parameter for a flat plate in terms of local reference-temperature conditions as obtained from the Blasius skin-friction relationship and Reynolds analogy is

$$\left(N'_{St}\sqrt{R'}\right)_l = \frac{0.664}{2\left(N'_{Pr}\right)^{2/3}}$$

A Prandtl number of 0.72 was assumed. The boundary-layer equations for axially symmetric flow over a sharp cone show that the local Stanton number is $\sqrt{3}$ times that for a flat plate in laminar flow for the same local Mach number, local Reynolds number, and ratio of wall temperature to local free-stream temperature (ref. 19).

Rewriting the laminar cone heat-transfer correlating parameter in terms of free-stream conditions, air being assumed, and solving for Stanton number results in

$$N_{St,\infty} = 2.493\sqrt{3}\,\frac{T_l^{1/4}}{p_\infty M_\infty}\sqrt{\frac{p_l M_l \mu' T_\infty}{T' x}}$$

where

$$\frac{T_\infty}{T_l} = \frac{1 + \frac{\gamma - 1}{2} M_l^2}{1 + \frac{\gamma - 1}{2} M_\infty^2}$$

and the reference temperature was taken from Monaghan's relation (ref. 20) $T'/T_l = 0.575\left(T_w/T_l\right) + 0.425 + 0.0328M_l^2$. Local conditions of temperature and Mach number were assumed to be cone surface conditions for a single conical shock which would raise the free-stream pressure to the measured local pressure.

Turbulent Strip Theory

From reference 21, the turbulent heating on a flat plate, in terms of local reference temperature conditions, is

$$\left[N'_{St}(R')^{1/5}\right]_l = \frac{0.0592}{2\left(N'_{Pr}\right)^{2/3}}$$

APPENDIX

Van Driest (ref. 19) shows that for a cone in axially symmetric flow, the local Stanton number is 1.15 times as great as that for a flat plate under the same local conditions. Rewriting the turbulent strip theory, air and $N_{Pr} = 0.72$ being assumed, for a cone results in the equation

$$N_{St,\infty} = 0.0765(1.15)\left(\frac{p_l M_l \sqrt{T_l}}{T'}\right)^{4/5} \frac{T_\infty}{p_\infty M_\infty}\left(\frac{\mu'}{x}\right)^{1/5}$$

The assumption of local flow conditions as for the laminar theory also was made, and the reference temperature was taken from Monaghan's relation for turbulent flow (ref. 22)

$$\frac{T'}{T_l} = 0.54\,\frac{T_w}{T_l} + 0.460 + 0.0284 M_l^{\,2}$$

REFERENCES

1. Deem, R. E.; Erickson, C. R.; and Murphy, J. S.: Flat-Plate Boundary-Layer Transition at Hypersonic Speeds. FDL-TDR-64-129 (Contract AF 33(657)-10660), U.S. Air Force, Oct. 1964. (Available from DDC as AD No. 453640.)

2. Sanator, R. J.; Savage, S. B.; DeCarlo, J. P.; Torrillo, D. T.; Casaccio, A.; and Cousin, S. B.: An Experimental and Theoretical Investigation of Inlets for Supersonic Combustion Ramjets – Parts I and II. Rept. No. RAC-480-63, Rep. Aviation Corp., June 1964.

3. Nagamatsu, H. T.; Graber, B. C.; and Sheer, R. E., Jr.: Combined Effects of Roughness, Bluntness, and Angle of Attack on Hypersonic Boundary Layer Transition – $M_1 \approx 8.5$ to 10.5. Rept. No. 65-C-011, Gen. Elec. Co., Sept. 1965.

4. Nagamatsu, H. T.; Graber, B. C.; and Sheer, R. E., Jr.: Laminar Cone Boundary Layer Transition – $M_1 = 10.2$ to 13.8. Rept. No. 65-C-005, Gen. Elec. Co., Oct. 1965.

5. Nagamatsu, H. T.; Graber, B. C.; and Sheer, R. E., Jr.: Hypersonic Laminar Boundary Layer Transition on 8-Foot Long 10° Cone. Rept. No. BSD-TR-65-471, Gen. Elec. Co., Dec. 1965.

6. Stainback, P. Calvin: Some Effects of Roughness and Variable Entropy on Transition at a Mach Number of 8. Paper No. 67-132, Am. Inst. Aeron. Astronaut., Jan. 1967.

7. Sanator, R. J.; DeCarlo, J. P.; and Torrillo, D. T.: Hypersonic Boundary-Layer Transition Data for a Cold-Wall Slender Cone. AIAA J., vol. 3, no. 4, Apr. 1965, pp. 758-760.

8. Staff of the Computing Section, Center of Analysis (Under Direction of Zdeněk Kopal): Tables of Supersonic Flow Around Cones. Tech. Rept. No. 1 (NOrd Contract No. 9169), Massachusetts Inst. Technol., 1947.

9. Chapman, Dean R.; and Rubesin, Morris W.: Temperature and Velocity Profiles in the Compressible Laminar Boundary Layer With Arbitrary Distribution of Surface Temperature. J. Aeron. Sci., vol. 16, no. 9, Sept. 1949, pp. 547-565.

10. Diaconis, N. S.; Jack, John R.; and Wisniewski, Richard J.: Boundary-Layer Transition at Mach 3.12 As Affected By Cooling and Nose Blunting. NACA TN 3928, 1957.

11. Wisniewski, Richard J.; and Jack, John R.: Recent Studies on the Effect of Cooling on Boundary-Layer Transition at Mach 4. J. Aerospace Sci. (Readers' Forum), vol. 28, no. 3, Mar. 1961, pp. 250-251.

12. Sheetz, Norman W., Jr.: Free-Flight Boundary Layer Transition Investigations at Hypersonic Speeds. AIAA Paper No. 65-127, Am. Inst. Aeron. Astronaut., Jan. 1965.

13. Nagamatsu, H. T.; Graber, B. C.; and Sheer, R. E., Jr.: Critical Layer Concept Relative to Hypersonic Boundary Layer Stability. Rept. No. 65-SD-829, Gen. Elec. Co., Feb. 1966.

14. James, Carlton S.: Observations of Turbulent-Burst Geometry and Growth in Supersonic Flow. NACA TN 4235, 1958.

15. Potter, J. Leith; and Whitfield, Jack D.: Boundary-Layer Transition Under Hypersonic Conditions. AEDC TR-65-99, U.S. Air Force, May 1965.

16. Van Driest, E. R.; and Boison, J. Christopher: Research on Stability and Transition of the Laminar Boundary Layer. Rept. No. AL-2196 (Contract AF 18(600)-786), North Am. Aviation, Inc., Sept. 1, 1955.

17. Brinich, Paul F.; and Sands, Norman: Effect of Bluntness on Transition for a Cone and a Hollow Cylinder at Mach 3.1. NACA TN 3979, 1957.

18. Laufer, John; and Marte, Jack E.: Results and a Critical Discussion of Transition-Reynolds-Number Measurements on Insulated Cones and Flat Plates in Supersonic Wind Tunnels. Rept. No. 20-96 (Contract No. DA-04-495-Ord 18), Jet Propulsion Lab., California Inst. Techn., Nov. 30, 1955.

19. Van Driest, E. R.: Turbulent Boundary Layer on a Cone in a Supersonic Flow at Zero Angle of Attack. J. Aeron. Sci., vol. 19, no. 1, Jan. 1952, pp. 55-57, 72.

20. Monaghan, R. J.: An Approximate Solution of the Compressible Laminar Boundary Layer on a Flat Plate. R. & M. No. 2760, Brit. A.R.C., 1953.

21. Schlichting, Hermann (j. Kestin, trans.): Boundary Layer Theory. McGraw-Hill Book Co., Inc., 1955.

22. Monaghan, R. J.: On the Behavior of Boundary Layers at Supersonic Speeds. Fifth International Aeronautical Conference (Los Angeles, Calif., June 20-23, 1955), Inst. Aeron. Sci., Inc., 1955, pp. 277-315.

TABLE I.- ORIFICE AND THERMOCOUPLE LOCATIONS

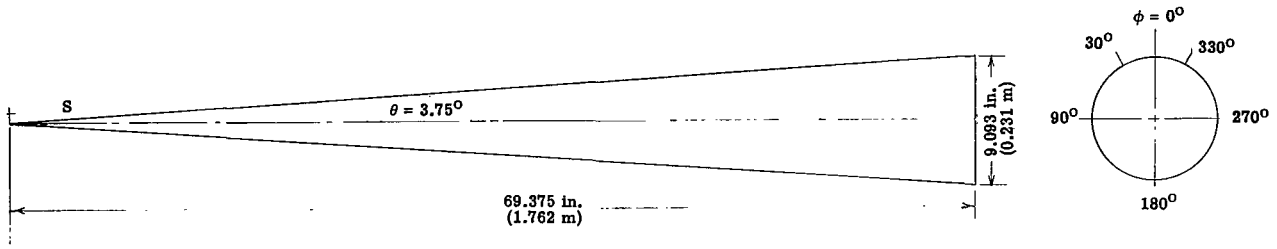

Thermocouple	S		φ, deg	Thermocouple	S		φ, deg	Orifice	S		φ, deg
	in.	m			in.	m			in.	m	
1	13.00	0.330	0	59	51.00	1.295	30	1	15.00	0.381	180
2	13.00	.330	90	60	52.00	1.321	330	2	20.00	.508	0
3	16.00	.406	0	61	52.00	1.321	0	3	20.00	.508	90
4	19.00	.483	0	62	52.00	1.321	30	4	20.00	.508	180
5	19.00	.483	90	63	53.00	1.346	330	5	25.00	.635	180
6	22.00	.559	0	64	53.00	1.346	0	6	30.00	.762	0
7	25.00	.635	0	65	53.00	1.346	30	7	30.00	.762	90
8	28.00	.711	0	66	53.75	1.365	180	8	30.00	.762	180
9	28.00	.711	90	67	54.00	1.372	330	9	35.00	.889	180
10	31.00	.787	0	68	54.00	1.372	0	10	40.00	1.016	180
11	32.50	.826	0	69	54.00	1.372	30	11	42.50	1.080	180
12	34.00	.864	0	70	55.00	1.397	330	12	45.00	1.143	180
13	35.50	.902	0	71	55.00	1.397	0	13	47.50	1.207	180
14	37.00	.940	330	72	55.00	1.397	30	14	50.00	1.270	180
15	37.00	.940	0	73	56.00	1.422	330	15	52.50	1.334	180
16	37.00	.940	30	74	56.00	1.422	0	16	55.00	1.397	180
17	37.00	.940	90	75	56.00	1.422	30	17	57.50	1.461	180
18	38.50	.978	330	76	56.75	1.441	180	18	60.00	1.524	180
19	38.50	.978	0	77	57.00	1.448	330	19	62.50	1.588	180
20	38.50	.978	30	78	57.00	1.448	0	20	65.00	1.651	180
21	40.00	1.016	330	79	57.00	1.448	30	21	67.50	1.715	180
22	40.00	1.016	0	80	58.00	1.473	330				
23	40.00	1.016	30	81	58.00	1.473	0				
24	40.00	1.016	90	82	58.00	1.473	30				
25	41.00	1.041	330	83	58.75	1.492	180				
26	41.00	1.041	0	84	59.00	1.499	330				
27	41.00	1.041	30	85	59.00	1.499	0				
28	42.00	1.067	330	86	59.00	1.499	30				
29	42.00	1.067	0	87	60.00	1.524	330				
30	42.00	1.067	30	88	60.00	1.524	0				
31	43.00	1.092	330	89	60.00	1.524	30				
32	43.00	1.092	0	90	60.00	1.524	90				
33	43.00	1.092	30	91	61.00	1.549	330				
34	44.00	1.118	330	92	61.00	1.549	0				
35	44.00	1.118	0	93	61.00	1.549	30				
36	44.00	1.118	30	94	62.00	1.575	330				
37	45.00	1.143	330	95	62.00	1.575	0				
38	45.00	1.143	0	96	62.00	1.575	30				
39	45.00	1.143	30	97	63.00	1.600	330				
40	46.00	1.168	330	98	63.00	1.600	0				
41	46.00	1.168	0	99	63.00	1.600	30				
42	46.00	1.168	30	100	63.75	1.619	180				
43	47.00	1.194	330	101	64.00	1.626	330				
44	47.00	1.194	0	102	64.00	1.626	0				
45	47.00	1.194	30	103	64.00	1.626	30				
46	48.00	1.219	330	104	65.00	1.651	330				
47	48.00	1.219	0	105	65.00	1.651	0				
48	48.00	1.219	30	106	65.00	1.651	30				
49	48.75	1.238	180	107	65.00	1.651	90				
50	49.00	1.245	330	108	66.00	1.676	330				
51	49.00	1.245	0	109	66.00	1.676	0				
52	49.00	1.245	30	110	66.00	1.676	30				
53	50.00	1.270	330	111	67.00	1.702	330				
54	50.00	1.270	0	112	67.00	1.702	0				
55	50.00	1.270	30	113	67.00	1.702	30				
56	50.00	1.270	90	114	68.00	1.727	330				
57	51.00	1.295	330	115	68.00	1.727	0				
58	51.00	1.295	0	116	68.00	1.727	30				

TABLE II.- TEST CONDITIONS

Stagnation pressure		Stagnation temperature		Free-stream Reynolds number	
psia	N/m^2	^oR	^oK	Per foot	Per meter
		Run 8			
299	20.615×10^5	1815	1008	0.394×10^6	1.293×10^6
354	24.407	1783	991	.490	1.608
401	27.648	1867	1037	.500	1.640
448	30.889	1833	1018	.584	1.916
503	34.681	1818	1010	.670	2.198
558	38.473	1795	997	.762	2.500
601	41.437	1817	1010	.803	2.635
651	44.885	1844	1025	.838	2.749
705	48.608	1816	1009	.943	3.094
759	52.331	1818	1010	1.019	3.343
801	55.227	1791	995	1.102	3.616
853	58.812	1797	998	1.163	3.816
903	62.260	1757	976	1.284	4.213
960	66.190	1786	992	1.330	4.364
		Run 9			
1059	73.015×10^5	1827	1015	1.370×10^6	4.495×10^6
		Run 10			
1119	77.152×10^5	1828	1016	1.385×10^6	4.544×10^6
1200	82.737	1834	1019	1.475	4.839
1297	89.425	1798	999	1.650	5.413
1392	95.975	1835	1020	1.728	5.669
1492	102.870	1846	1026	1.830	6.004
1583	109.144	1811	1006	2.002	6.568
1771	122.106	1822	1012	2.232	7.323

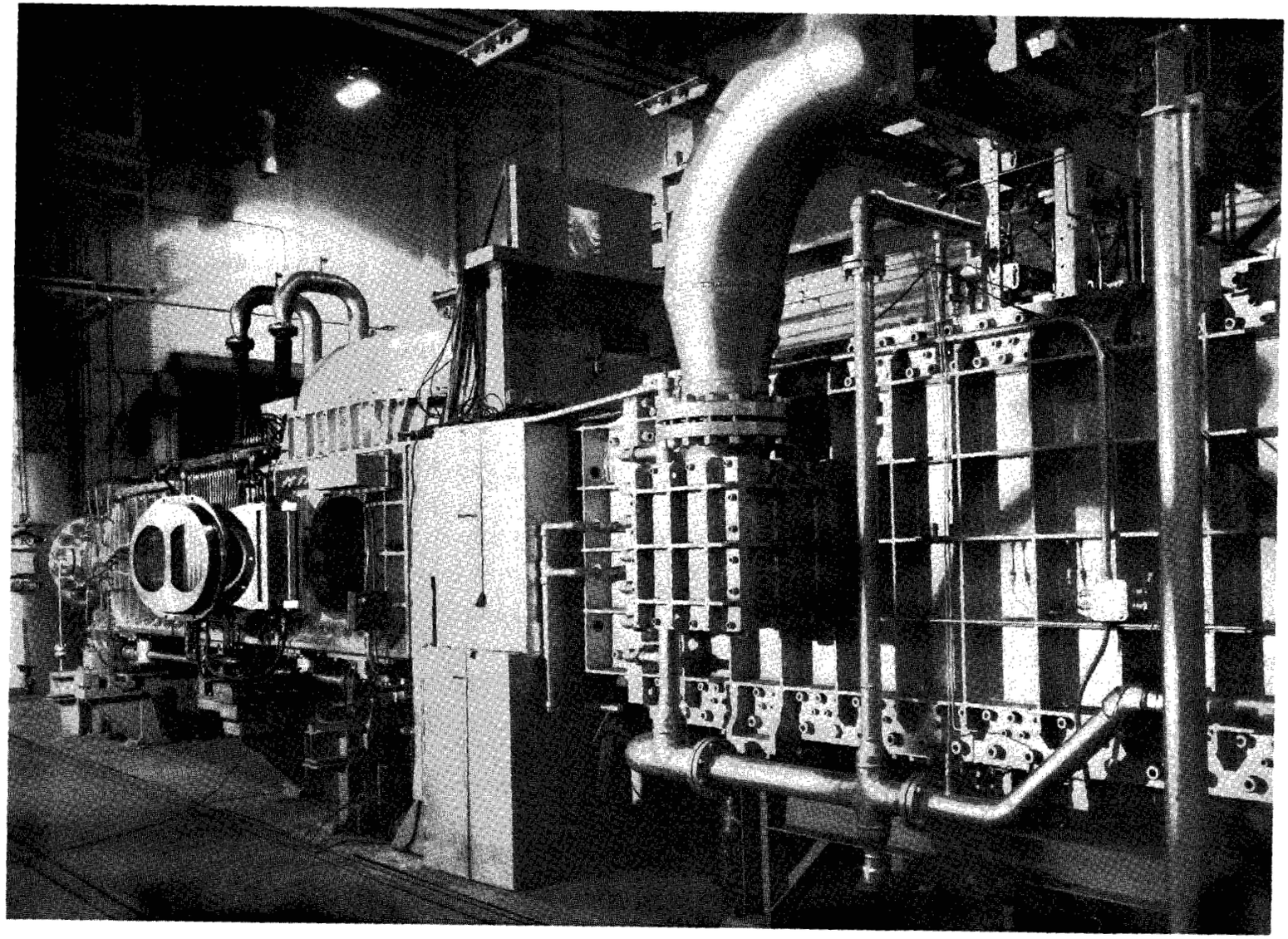

Figure 1.- Photograph of test facility.

L-65-5822

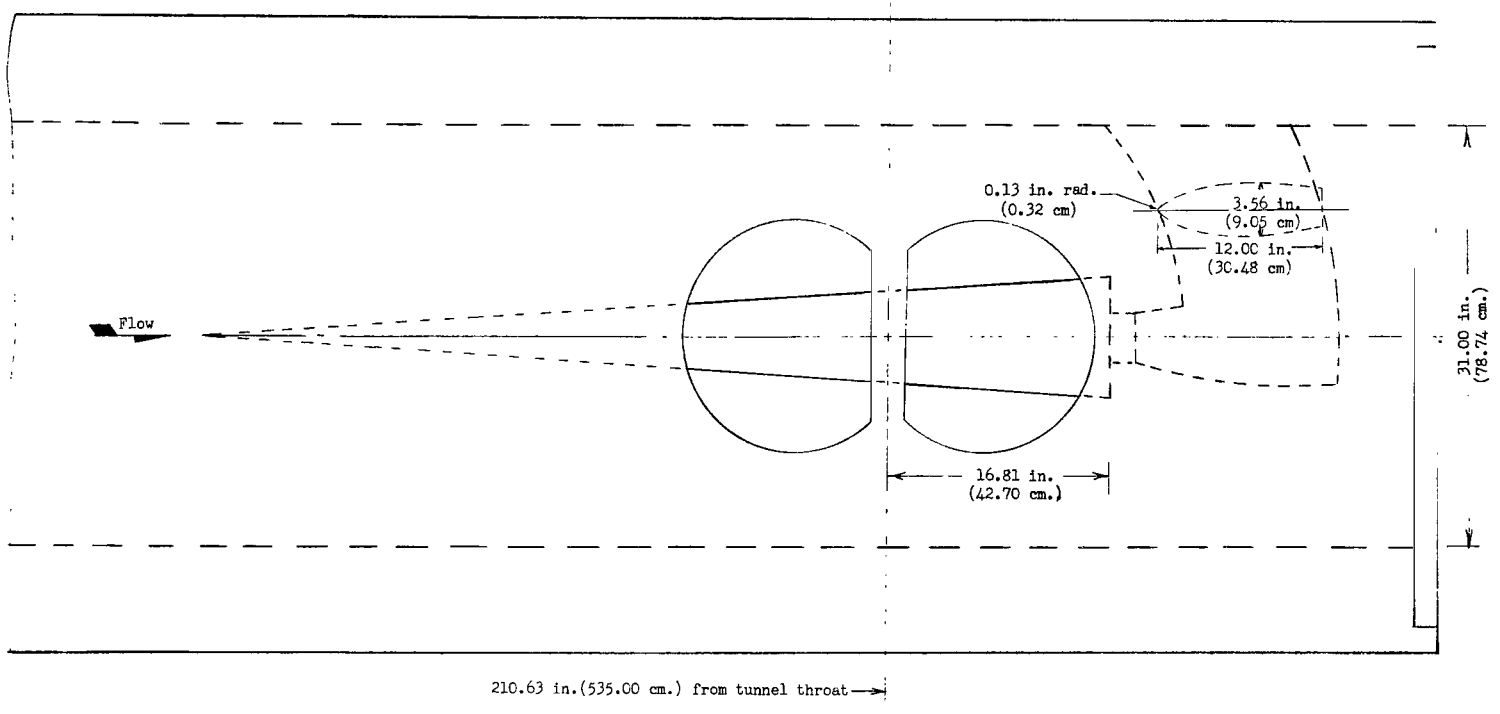

Figure 2.- Sketch of typical installation of cone model in tunnel.

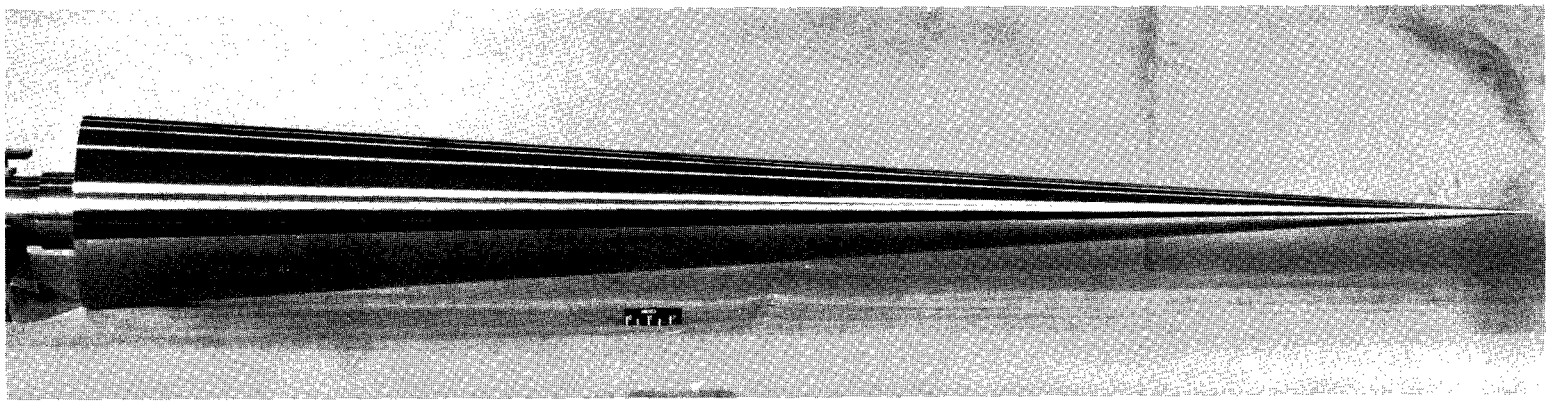

(a) Photograph of basic model. L-62-5933

Figure 3.- Cone used in investigation.

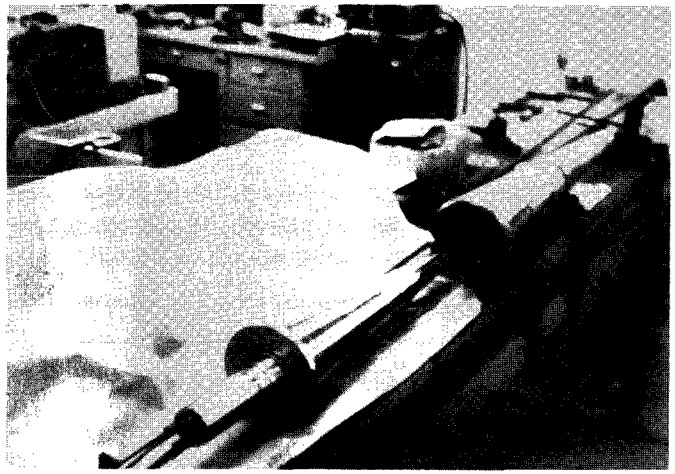

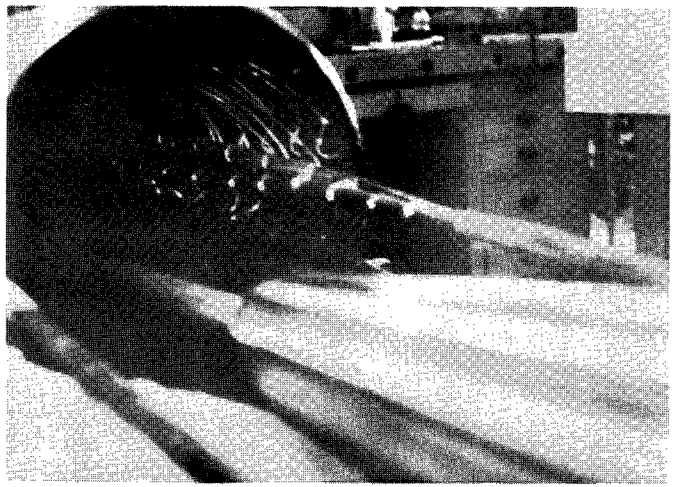

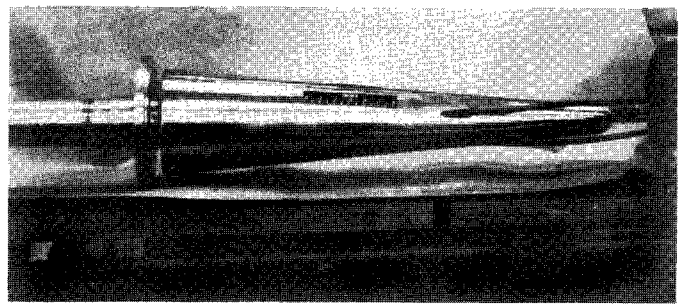

(b) Model construction. L-67-1055

Figure 3.- Concluded.

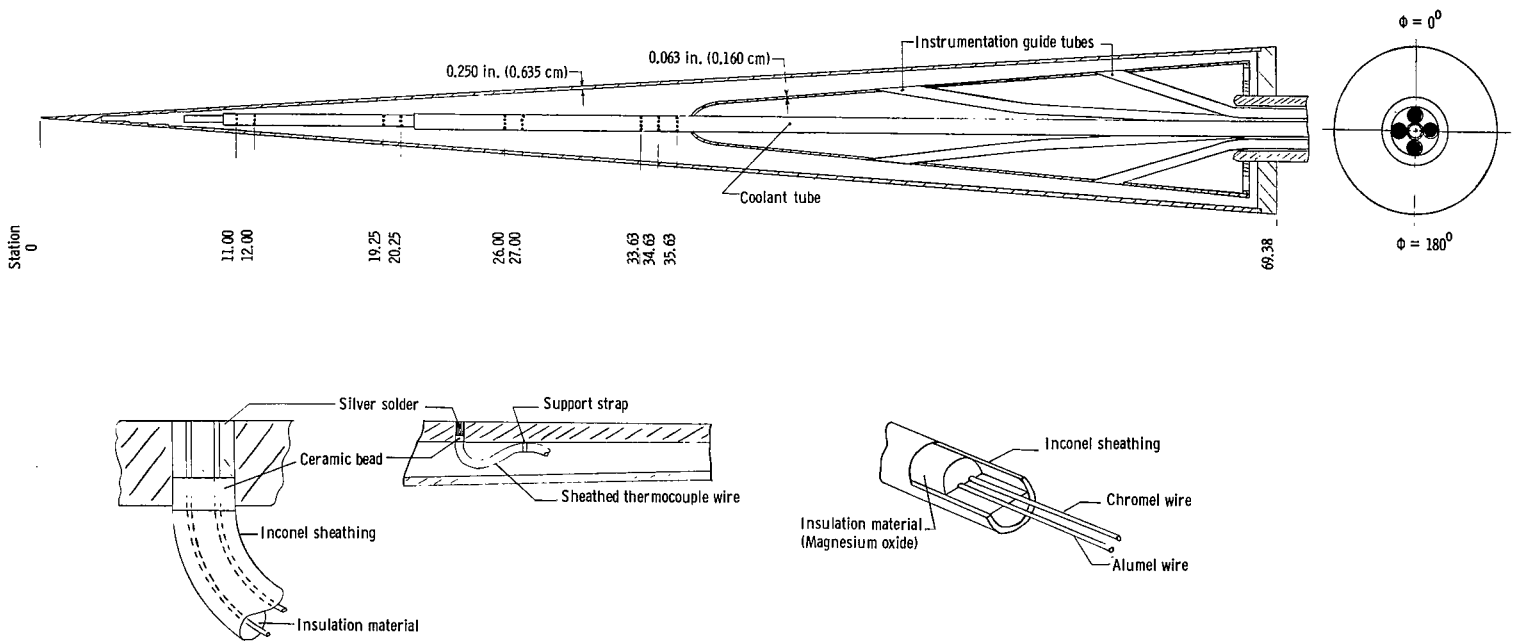

Figure 4.- Sketch of cone showing coolant tube and thermocouple installation.

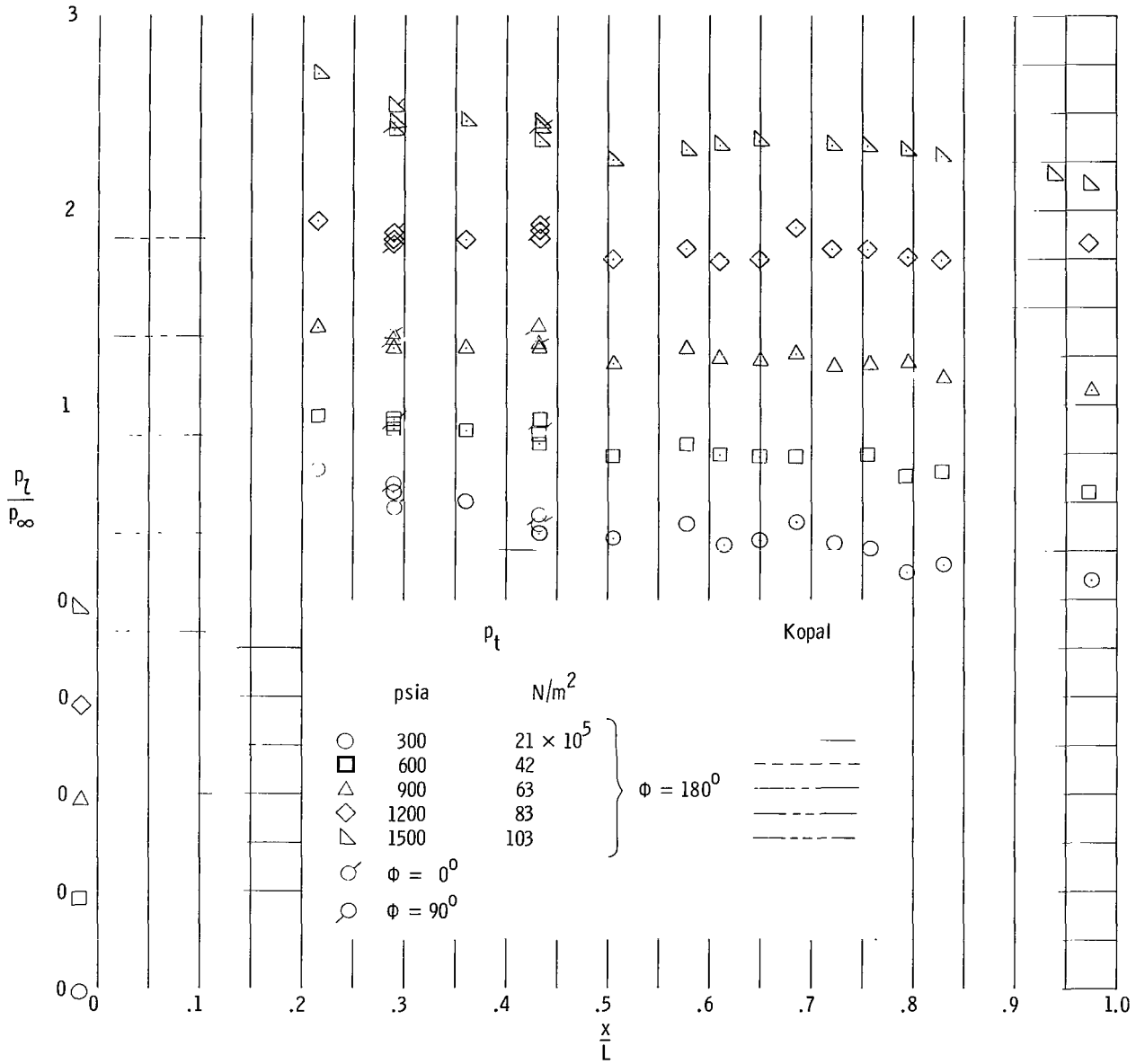

Figure 5.- Pressure distribution along the cone surface.

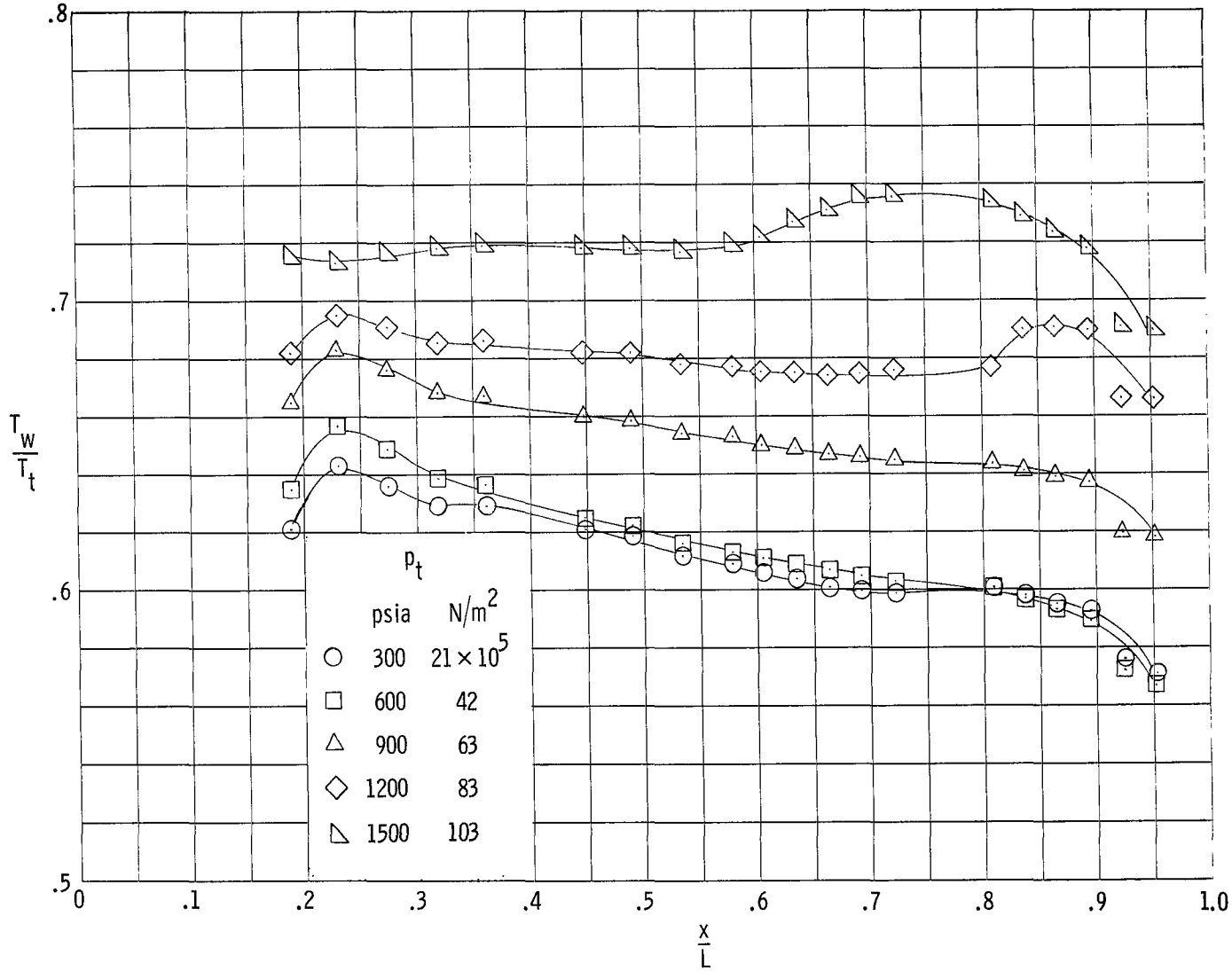

(a) Wall equilibrium temperature distribution.

Figure 6.- Temperature distribution along cone surface.

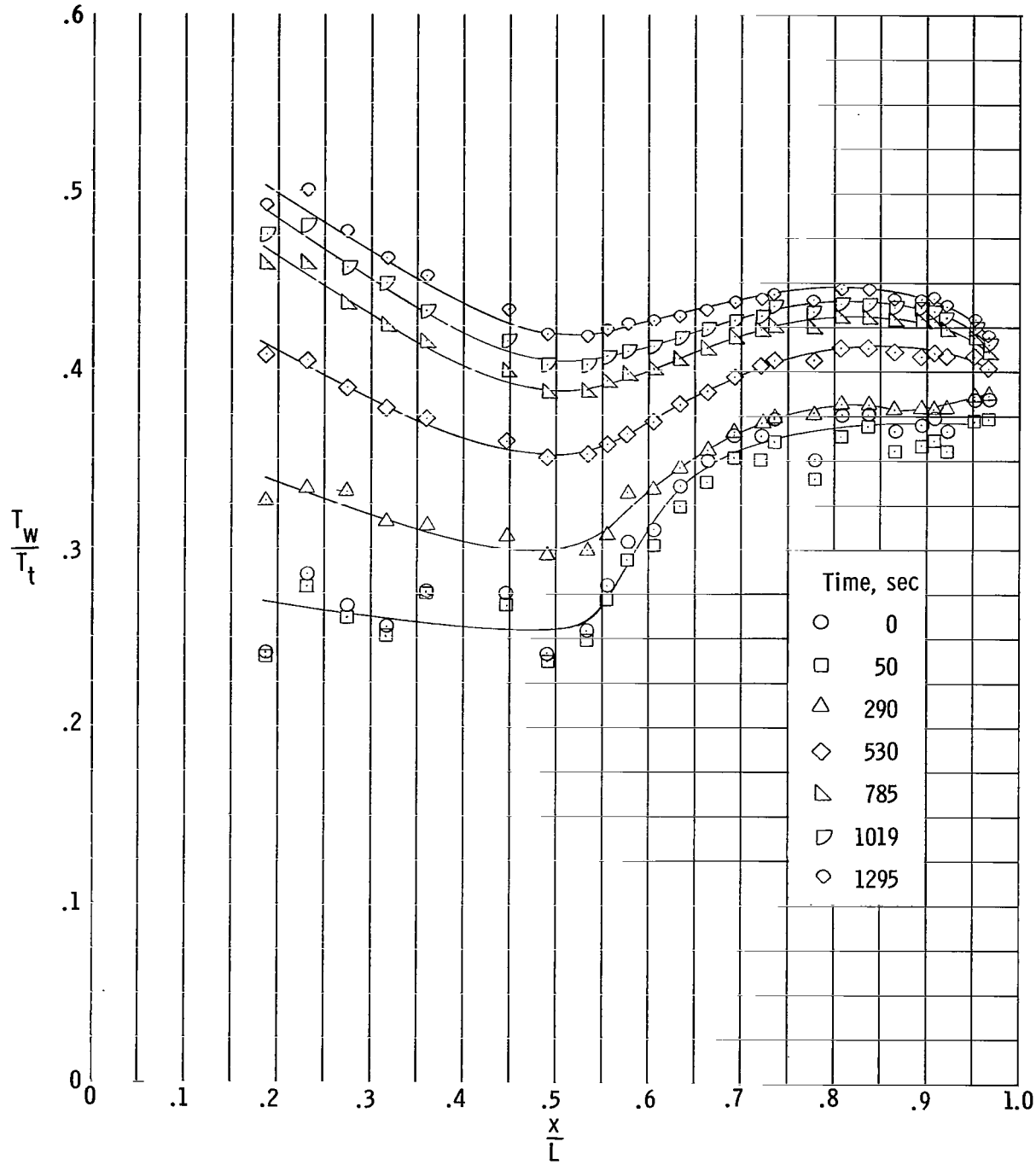

(b) Variation of cone wall temperature at 300 psia.

Figure 6.- Continued.

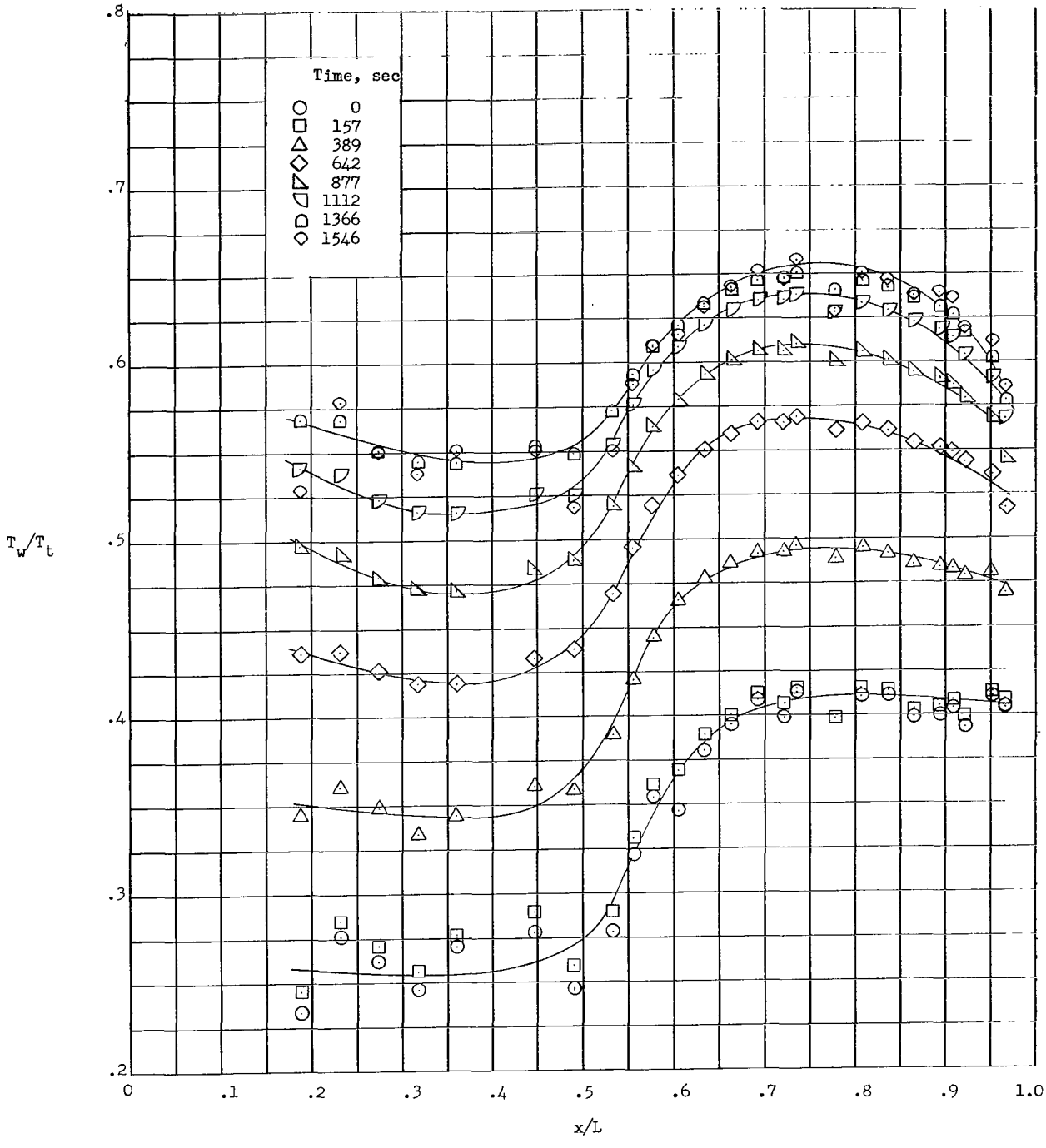

(c) Variation of cone wall temperature at 1500 psia.

Figure 6.- Concluded.

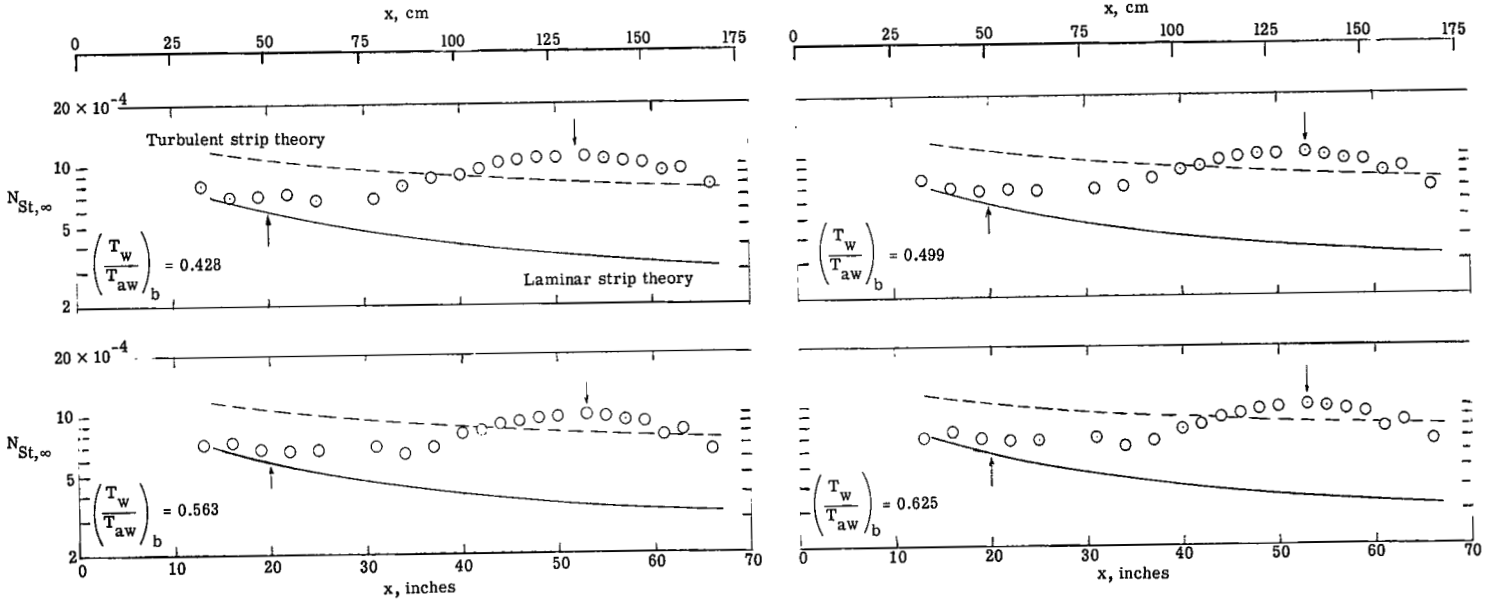

(a) Stanton number distribution at $R_1/ft = 2.7 \times 10^6$ (8.86×10^6 per meter).

Figure 7.- Effect of wall temperature on transition on sharp cone.

Symbol	Reference	θ, deg	M_ℓ	Unit Reynolds number R_ℓ/ft	Unit Reynolds number R_ℓ/m	Method of detecting transition
○	Present data	3.75	8.9	2.7×10^6	8.9×10^6	Heat transfer (end of transition)
○	Present data	3.75	8.9	2.7	8.9	Heat transfer (start of transition)
□	7	5.00	8.9	2.7	8.9	Heat transfer (end of transition)
□	7	5.00	8.9	2.7	8.9	Heat transfer (start of transition)
◇	10	9.50	3.0	7.2	24.0	Rate of temperature rise (start of transition)
△	11	13.50	3.5	10.0	33.0	Rate of temperature rise (start of transition)
◺	12	5.00	4.3 - 4.8	21.0 - 22.0	69.0 - 72.0	Spark shadowgraph
◹	12	5.00	3.0 - 3.1	13.0 - 15.0	43.0 - 49.0	Spark shadowgraph

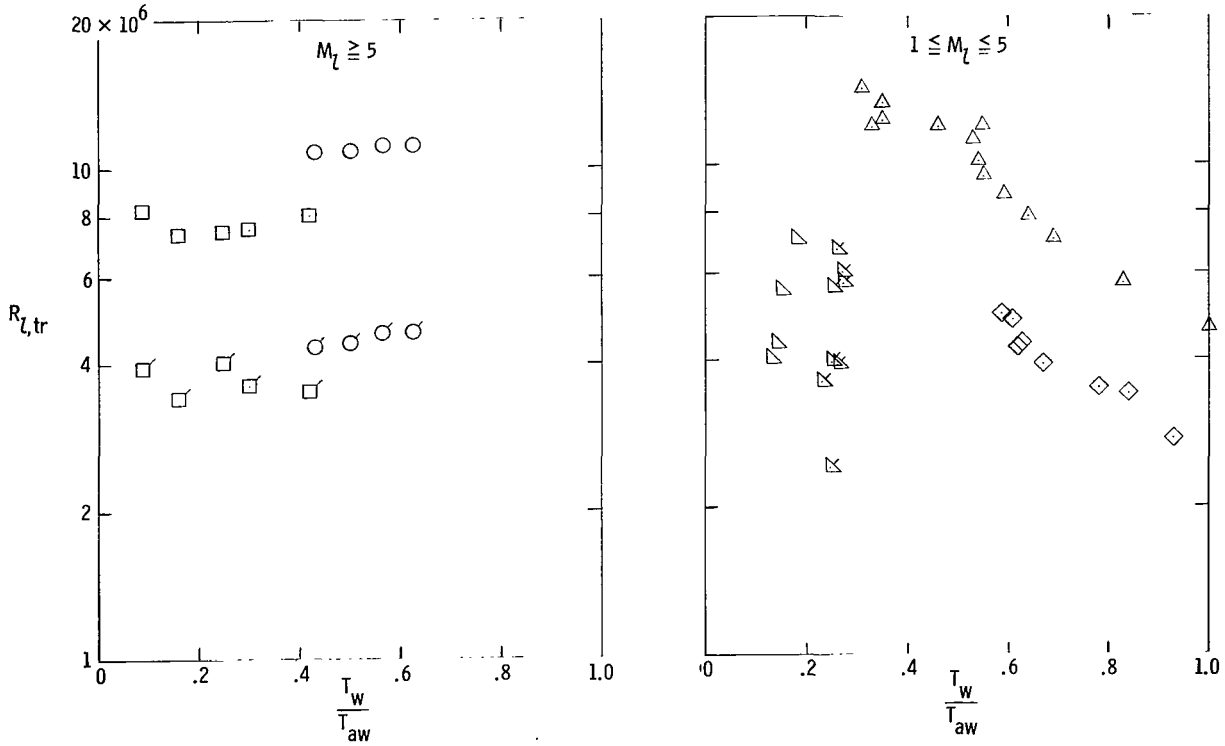

(b) Effect of T_w/T_{aw} on local transition Reynolds number.

Figure 7.- Concluded.

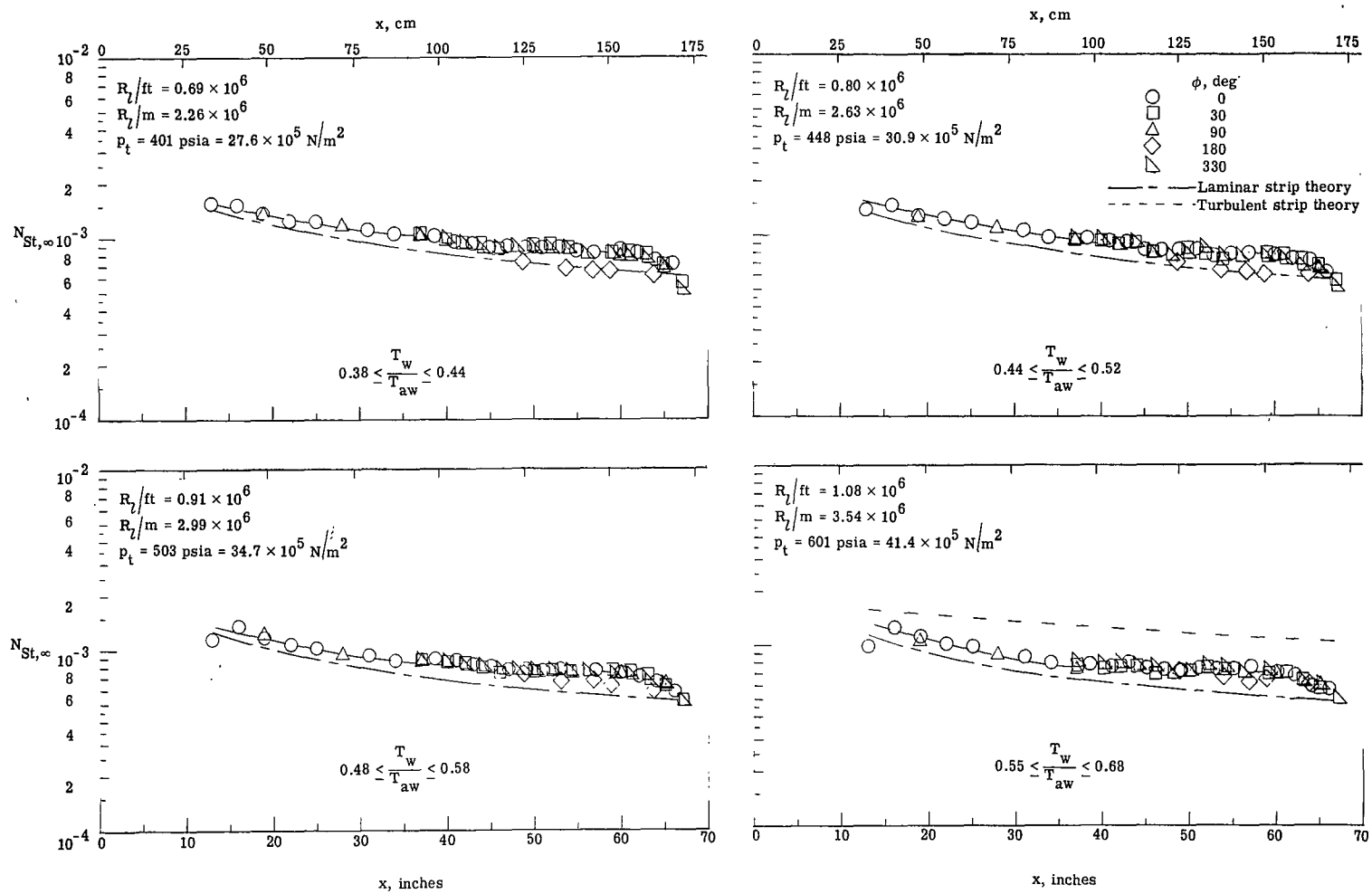

(a) Local unit Reynolds numbers from 0.69×10^6 to 1.08×10^6 per foot (2.26×10^6 to 3.54×10^6 per meter).

Figure 8.- Stanton number distribution.

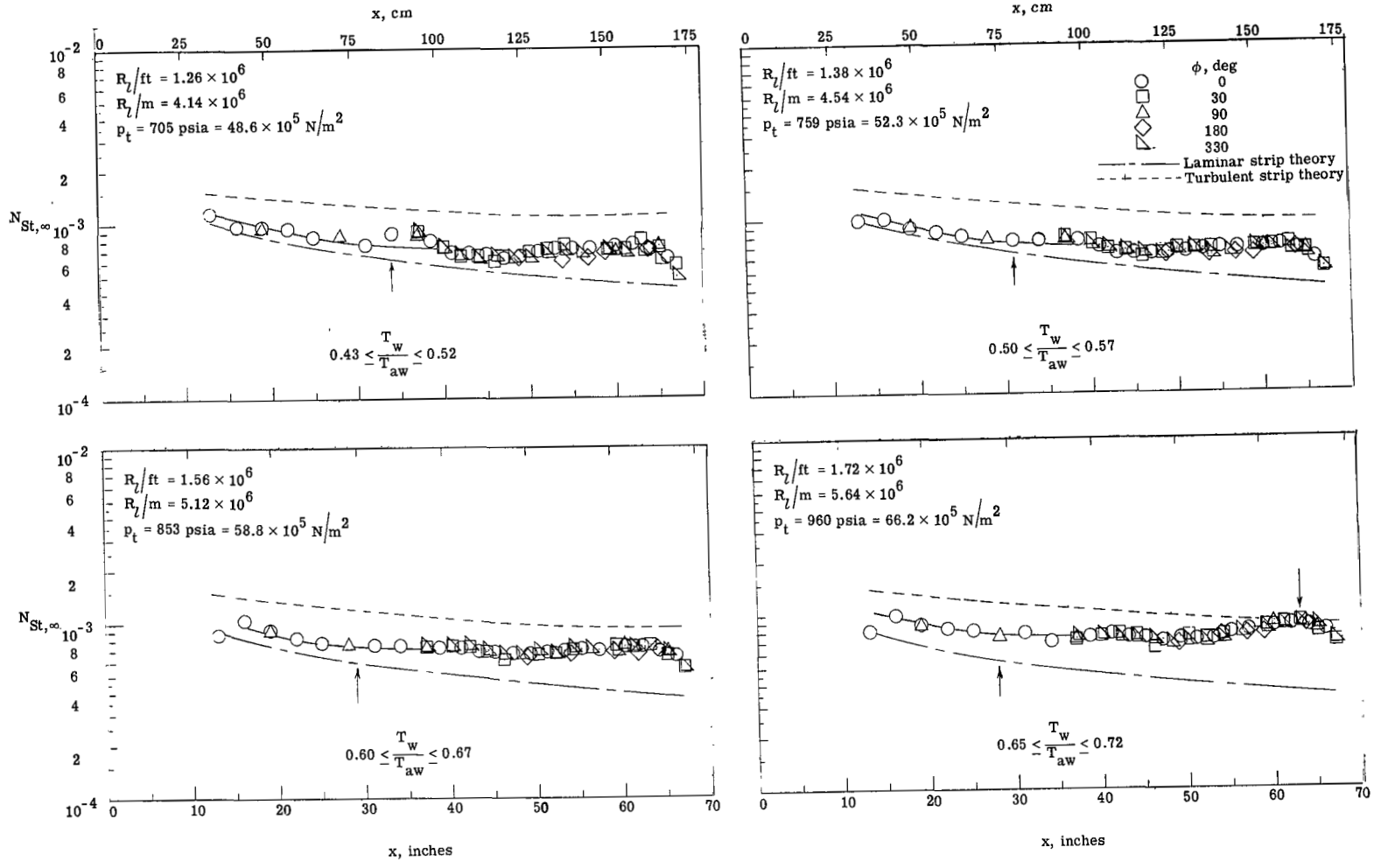

(b) Local unit Reynolds numbers from 1.26×10^6 to 1.72×10^6 per foot (4.13×10^6 to 5.64×10^6 per meter).

Figure 8.- Continued.

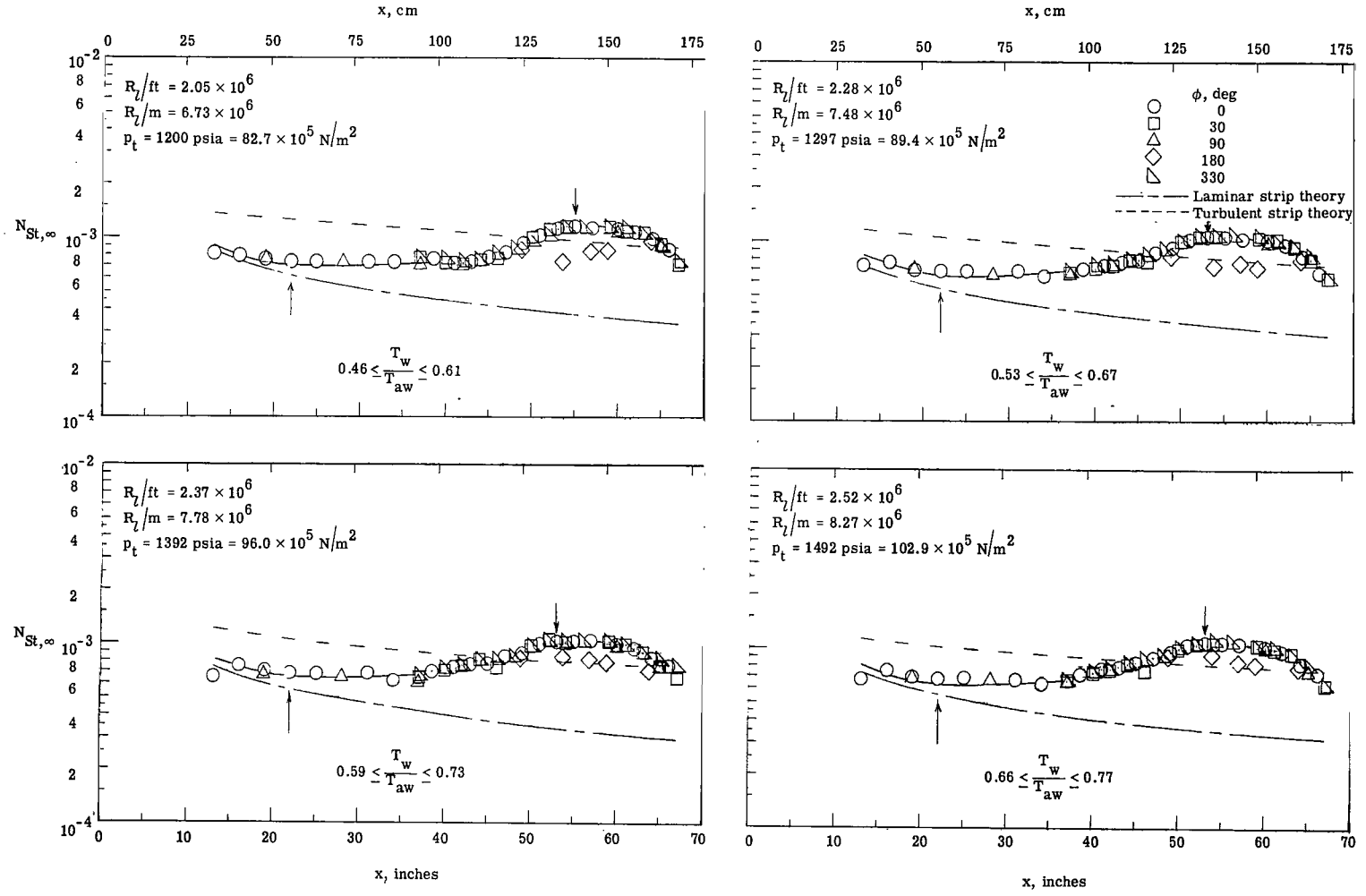

(c) Local unit Reynolds numbers from 2.05×10^6 to 2.52×10^6 per foot (6.73×10^6 to 8.27×10^6 per meter).

Figure 8.- Continued.

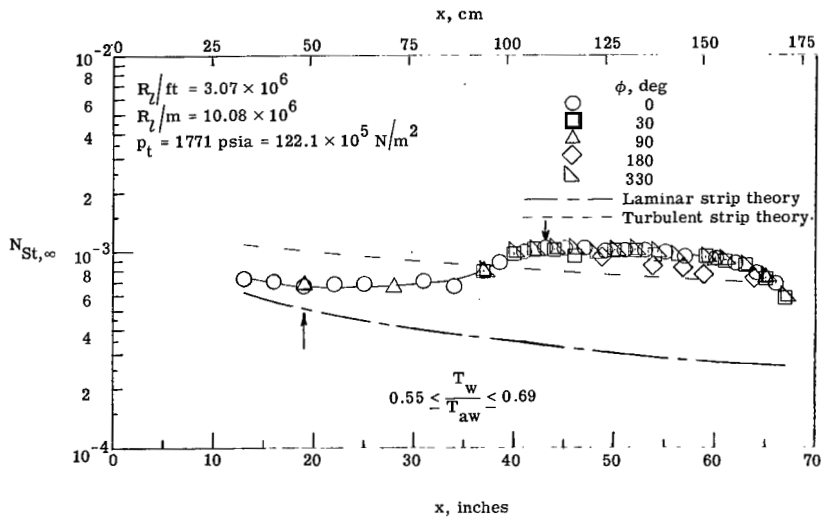

(d) Local unit Reynolds number of 3.07 × 10^6 per foot (10.07 × 10^6 per meter).

Figure 8.- Concluded.

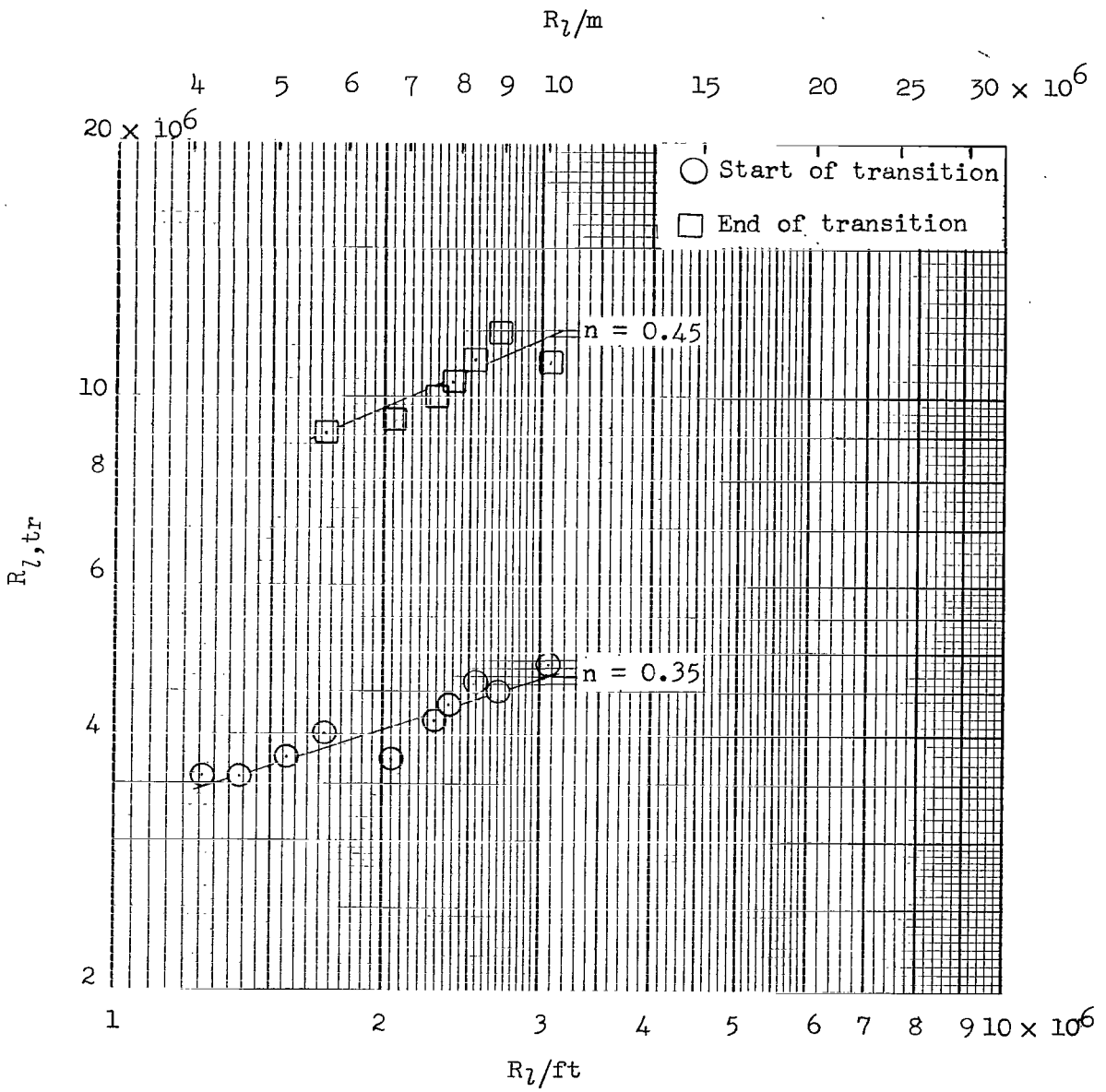

Figure 9.- Variation of local transition Reynolds number with local unit Reynolds number at $M_l \approx 9.0$.

Symbol	Reference	θ, deg	Unit Reynolds Number R_l/ft	Unit Reynolds Number R_l/m	Method of Detecting Transition
○	Present data	3.75	2.5×10^6	8.2×10^6	Heat transfer (end of transition)
⊙	Present data	3.75	2.4	7.9	Heat transfer (end of transition)
□	7	5.00	2.7	8.9	Heat transfer (end of transition)
◇	15	5.00	2.4	7.9	Shadowgraph
△	16	5.00	2.4	7.9	Magnified schlieren
◸	17	5.00	2.4	7.9	Peak surface temperature
◡	18	2.50	2.4	7.9	Peak surface temperature

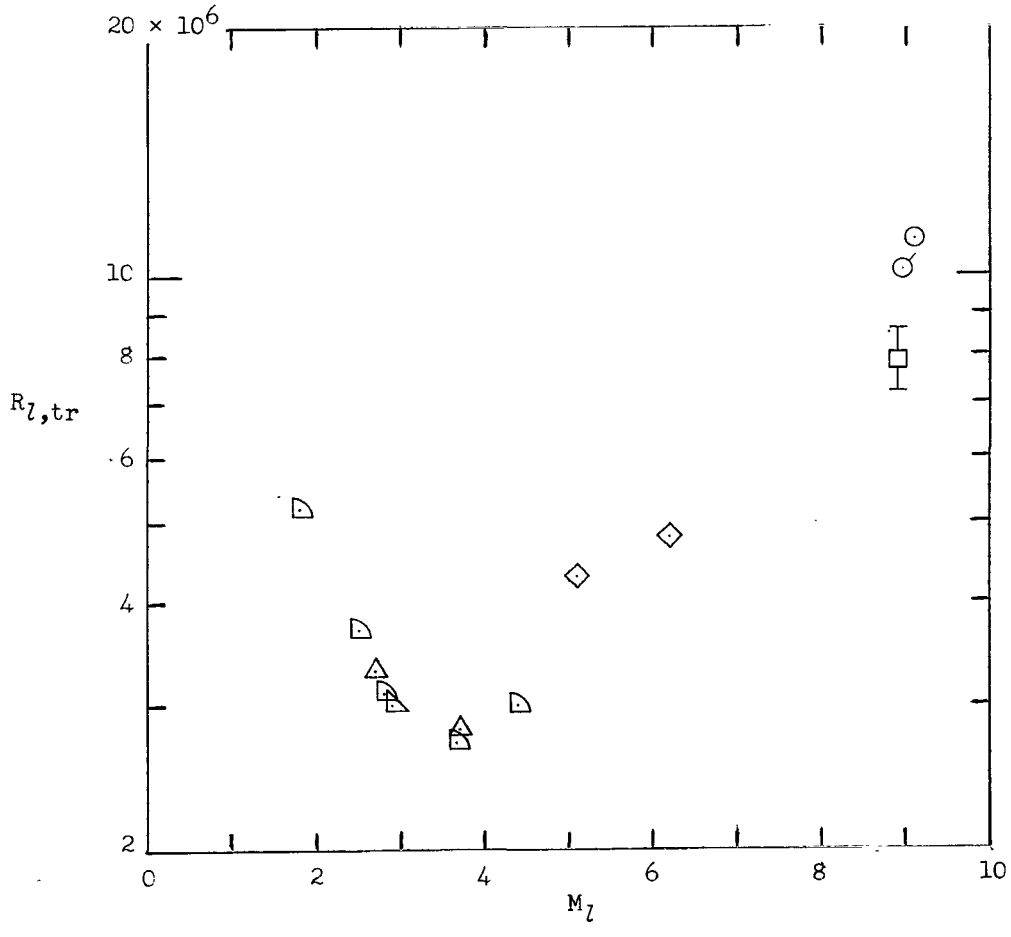

Figure 10.- The qualitative effect of local Mach number on local transition Reynolds number on sharp cones and angle of attack of 0^0.

"The aeronautical and space activities of the United States shall be conducted so as to contribute . . . to the expansion of human knowledge of phenomena in the atmosphere and space. The Administration shall provide for the widest practicable and appropriate dissemination of information concerning its activities and the results thereof."

—NATIONAL AERONAUTICS AND SPACE ACT OF 1958

NASA SCIENTIFIC AND TECHNICAL PUBLICATIONS

TECHNICAL REPORTS: Scientific and technical information considered important, complete, and a lasting contribution to existing knowledge.

TECHNICAL NOTES: Information less broad in scope but nevertheless of importance as a contribution to existing knowledge.

TECHNICAL MEMORANDUMS: Information receiving limited distribution because of preliminary data, security classification, or other reasons.

CONTRACTOR REPORTS: Scientific and technical information generated under a NASA contract or grant and considered an important contribution to existing knowledge.

TECHNICAL TRANSLATIONS: Information published in a foreign language considered to merit NASA distribution in English.

SPECIAL PUBLICATIONS: Information derived from or of value to NASA activities. Publications include conference proceedings, monographs, data compilations, handbooks, sourcebooks, and special bibliographies.

TECHNOLOGY UTILIZATION PUBLICATIONS: Information on technology used by NASA that may be of particular interest in commercial and other non-aerospace applications. Publications include Tech Briefs, Technology Utilization Reports and Notes, and Technology Surveys.

Details on the availability of these publications may be obtained from:

SCIENTIFIC AND TECHNICAL INFORMATION DIVISION

NATIONAL AERONAUTICS AND SPACE ADMINISTRATION

Washington, D.C. 20546